ELSEVIER

Journal of Alloys and Compounds 408–412 (2006) 490–495

Journal of ALLOYS AND COMPOUNDS

www.elsevier.com/locate/jallcom

Synthesis and characterization of a family of two related quaternary selenides: $Na_8Eu_2(Si_2Se_6)_2$ and $Na_9Sm(Ge_2Se_6)_2$

Benjamin R. Martin, Larisa A. Polyakova, Peter K. Dorhout *

Department of Chemistry, Colorado State University, Fort Collins, CO 80523-1872, USA

Received 30 July 2004; received in revised form 13 December 2004; accepted 15 December 2004
Available online 13 June 2005

Abstract

In this work, two related quaternary rare earth selenide phases were synthesised using the molten flux method. $Na_8Eu_2(Si_2Se_6)_2$ crystallizes in *C*2/*m* with cell parameters $a = 7.0898(10)$ Å, $b = 12.228(2)$ Å, $c = 7.9499(11)$ Å, $\beta = 107.427(2)^\circ$ and $V = 657.6(2)$ Å^3 ($Z = 1$). This structure comprises layers of $[Eu_2(Si_2Se_6)_2]^{8-}$ that are in the (1 1 0) planes; each contains ethane-like $(Si_2Se_6)^{6-}$ units oriented along *c*, or perpendicular to the planes. This phase is reminiscent of the family of $M_2P_2S_6$ well-known layered phases and we prepared the series where the main group metal was Si or Ge and the chalcogen was Se or Te. $Na_9Sm(Ge_2Se_6)_2$ is a related structure, also crystallizing in *C*2/*m* with cell parameters $a = 7.9158(15)$ Å, $b = 12.244(2)$ Å, $c = 7.1048(13)$ Å, $\beta = 106.99(1)^\circ$ and $V = 658.6(2)$ Å^3 ($Z = 1$). This structure comprises layers of $[Sm_2(Ge_2Se_6)_2]^{9-}$ similar to the selenosilicate yet contains ethane-like $(Ge_2Se_6)^{6-}$ units oriented along *a*, i.e. parallel to the layers. We have investigated the family of solids changing the chalcogen atoms (S, Se and Te) and evaluating how the structure changes with chalcogen and with the tetrelide atom (Ge, Si). In addition to single crystal diffraction studies, Raman, diffuse reflectance UV–vis and photoluminescence measurements (for Eu phases) have been used to characterize these compounds.

Keywords: Molten flux; Chalcogenide; Crystallography; Lanthanide; Quaternary

1. Introduction

The synthesis and study of complex structures containing four or more elements in unique coordination environments remains at the frontier of inorganic chemistry. The sheer number of possible structures makes the study of such materials a daunting task. Hypothesis-driven synthesis is necessary in order to organize searches and to generate reasonable conclusions about resulting structures. However, some degree of knowledge about possible organizations of structural components is necessary before such searches are possible.

Quaternary structures resulting from the combination of alkali metals, transition or rare earth metals, main group elements and heavy chalcogens (sulfur, selenium or tellurium) represent a versatile category of materials that have received a great deal of recent attention. These structures can be treated as main group chalcogenide units that are linked together through the metal cations. The structural versatility of main group chalcogenide units known from ternary structures is encouraging, with geometries ranging from tetrahedral, as in $(GeSe_4)^{4-}$, to the ethane-like $(Ge_2Se_6)^{6-}$, to the adamantane-like $(Ge_4Se_{10})^{4-}$ [1–3]. Unit stoichiometries and predictions based on charge balance can be used to determine reactant stoichiometries that may generate stable structures. Examples of quaternary structures containing main group chalcogenide units include $KLaGeSe_4$ [4], $Na_8Pb_2(Si_2Se_6)_2$ [5] and a family of potassium lanthanum selenophosphates [6].

Many methods have been used to prepare chalcogenide structures, but reactive flux synthesis has proven to be one of the most successful methods [7]. Using this method, low-melting alkali chalcogenide Zintl ions are used as both solvents and reactants under moderate reaction conditions. This flux can be composed of any alkali metal with S, Se or Te, and the melting point and oxidative power of the flux can be

* Corresponding author.
E-mail address: Peter.Dorhout@colostate.edu (P.K. Dorhout).

0925-8388/$ – see front matter © 2005 Elsevier B.V. All rights reserved.
doi:10.1016/j.jallcom.2004.12.091

adjusted by adjusting the stoichiometry of the salt. Reactions that take place in a reactive flux benefit from increased diffusion, allowing reactions to take place at a lower temperature. Enhanced single crystal growth can be achieved by allowing the solution to cool slowly, and the resulting crystals can be isolated by dissolving the remaining flux.

In this paper, two different layered quaternary structures prepared using the reactive flux method are reported. These structures both contain ethane-like main group selenide $M_2Se_6^{6-}$ (M = Si, Ge) units interconnected with lanthanide cations. $Na_8Eu_2(Si_2Se_6)_2$ is nearly isostructural with $Na_8Pb_2(Si_2Se_6)_2$ [5]. $Na_9Sm(Ge_2Se_6)_2$ is a new structure, but it is closely related to $Na_8Eu_2(Si_2Se_6)_2$. To the authors' knowledge, $Na_9Sm(Ge_2Se_6)_2$ is the first published example of a quaternary structure containing Ge_2Se_6 units, but it has come to our attention that Kanatzidis et al. have synthesised two germanium selenide structures closely related to $Na_8Pb_2(Si_2Se_6)_2$, $Na_8Pb_2(Ge_2Se_6)_2$ and $K_8Pb_2(Ge_2Se_6)_2$ [8]. Raman, photoluminescence and diffuse reflectance UV–vis spectroscopic characterization are also discussed.

2. Experimental

2.1. Synthesis

The following reagents were used as received and stored in a nitrogen atmosphere glovebox: Sm, Eu, La (99.95%, Ames Laboratory), Ge (99.999%, Cerac), Si (99.999%, Johnson–Matthey) and Se or Te (99.999%, Johnson–Matthey). Na_2Te_3 or Na_2Se_2 were previously made in liquid ammonia from stoichiometric combination of the elements. Reactants were loaded into fused silica ampoules inside an inert atmosphere glovebox, each ampoule was flame sealed under vacuum, and placed in a temperature controlled furnace. After the reactions were complete, the ampoules were opened, and the products were washed with *N*,*N*-dimethylformamide (DMF) to remove unreacted flux.

$Na_8Eu_2(Si_2Se_6)_2$ **I**, was synthesised by combining 45.8 mg (0.301 mmol) of Eu, 123.4 mg (0.605 mmol) of Na_2Se_2, 65.4 mg (0.828 mmol) of Se and 21.7 mg (0.773 mmol) of Si. Compound **I** was ramped to 750 °C, at 35 °C/h, where it remained for 150 h. The sample was cooled to room temperature at 3 °C/h, yielding orange-brown plate-like crystals of $Na_8Eu_2(Si_2Se_6)_2$. Semiquantitative energy dispersive analysis (EDS) using a scanning electron microscope on a number of orange-brown plates confirmed the presence and stoichiometry of all four elements.

$Na_9Sm(Ge_2Se_6)_2$ **II**, was synthesised by combining 28.3 mg Sm (mmol), 83.3 mg Ge (mmol), 60.0 mg Se (mmol) and 159.8 mg Na_2Se_2 (mmol). Compound **II** was ramped to 725 °C at 35 °C/h, where it remained for 150 h. The sample was cooled to room temperature at a rate of 4 °C/h, yielding ruby-red plates of $Na_9Sm(Ge_2Se_6)_2$ intergrown with yellow plates of $Na_8Ge_4Se_{10}$ and other ternary sodium germanium selenides. EDS analysis of the red crystals confirmed the presence and stoichiometry of all four elements.

2.2. Physical measurements

2.2.1. Single crystal X-ray diffraction

Intensity data sets for compounds **I** and **II** were collected using a Bruker Smart CCD diffractometer equipped with a graphite monochrometer and a Mo Kα radiation source. These data were integrated using SAINT [9], a SADABS correction was applied [10], and the structures were solved by direct methods using SHELXTL [11]. Crystallographic data for compounds **I** and **II** are reported in Table 1.

2.2.2. Raman spectroscopy

The solid-state Raman spectra of compounds **I** and **II** were taken with a Nicolet Magna-IR spectrometer with FT-Raman module attachment using Nd:YAG excitation laser (1064 nm).

2.2.3. UV–vis spectroscopy

Diffuse reflectance measurements on **I** were taken with Varian Cary 500 Scan UV–vis–near-IR spectrophotometer equipped with a Praying Mantis accessory. A polyteflon standard was used as a reference. The Kubelka–Munk function was applied to obtain band gap information [12–14].

2.2.4. Photoluminescence spectroscopy

The solid-state photoluminescence excitation and emission spectra of compound **I** were taken on a SPEX Fluorlog-3 spectrofluorometer using bulk crystals at room temperature.

2.3. Structure determination

2.3.1. $Na_8Eu_2(Si_2Se_6)_2$ *I*

A plate-like crystal of $Na_8Eu_2(Si_2Se_6)_2$ with dimensions 0.03 mm × 0.06 mm × 0.09 mm was mounted on a glass fiber with epoxy. Cell constants were initially calculated from 120 frames of reflections. The final cell constants were determined from a set of 2109 strong reflections. A SADABS absorption correction was applied (R_{int} = 0.0362) and all atoms were refined anisotropically on F^2 for 38 variables [11]. Systematic absences and Friedel pair comparisons pointed clearly to the space group *C*2/*m*. Table 2 lists fractional coordinates and equivalent isotropic displacement parameters for $Na_8Eu_2(Si_2Se_6)_2$, and Fig. 1a displays anisotropic displacement ellipsoids for the major component of the structure.

Compound **I** was modeled as a disordered structure consisting of occupational disorder at a shared sodium/europium site, as illustrated in Fig. 2. The initial structure determination was based upon a single europium site, and a single crystallographically unique sodium site. However, the atomic displacement parameter, *U*(eq) of Eu(1) was high (0.054 Å^2), compared to the other atoms. When this position was assigned as 100% sodium, the atomic displacement parameter was

Table 1
Crystallographic data for $Na_8Eu_2(M_2Q_6)_2$ (M = Ge, Si; Q = Se, Te) and $Na_9RE(M_2Se_6)_2$ (RE = Sm, La; M = Ge, Si)[a]

Compound	$Na_8Eu_2(Si_2Se_6)_2$ **I**	$Na_8Eu_2(Ge_2Se_6)_2$	$Na_8Eu_2(Si_2Te_6)_2$	$Na_9Sm(Si_2Se_6)_2$	$Na_9Sm(Ge_2Se_6)_2$ **II**	$Na_9La(Ge_2Se_6)_2$
Formula weight	1547.72	1725.72	2131.40	1417.14	1595.14	1583.70
a (Å)	7.0898(10)	7.1388(16)	7.6466(10)	7.0052(11)	7.9158(15)	7.9726(8)
b (Å)	12.2280(16)	12.334(3)	13.2195(17)	12.0852(18)	12.244(2)	12.3349(13)
c (Å)	7.9499(11)	8.0195(18)	8.4371(11)	7.9130(12)	7.1048(13)	7.1121(7)
β (°)	107.427(2)	107.267(4)	107.662(2)	107.200(3)	106.993(3)	107.112(2)
V (Å^3)	657.57(16)	674.3(3)	812.66(18)	639.95(17)	658.6(2)	668.45(12)
ρ_{calcd} (g/cm^3)	3.908	4.250	4.355	3.677	4.022	3.934
μ (mm^{-1})	21.638	25.295	14.630	19.690	23.428	22.482
R^b (%)	2.10	2.28	2.03	4.18	2.09	1.84
R_w[b] (%)	4.93	5.54	4.24	9.03	4.78	4.23

[a] For all structures $Z = 1$, space group = $C2/m$, $T = 298(2)$ K and λ(Mo Kα) = 0.71073 Å.

[b] $R = \sum |F_o| - |F_c| / \sum |F_o|$, $R_w = \left[\sum [w(F_o^2 - F_c^2)^2] / \sum [w(F_o^2)^2]\right]^{1/2}$.

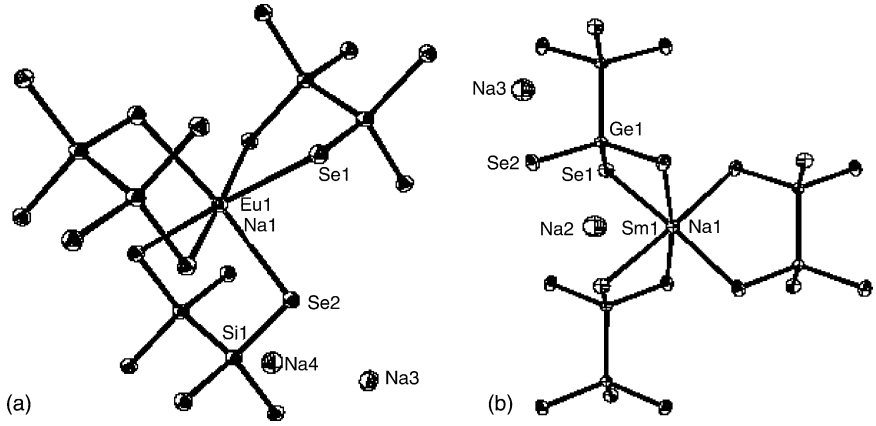

Fig. 1. Ellipsoid plots displaying anisotropic displacement ellipsoids at 50% probability of the major component of (a) $Na_8Eu_2(Si_2Se_6)_2$ and (b) $Na_9Sm(Ge_2Se_6)_2$.

almost zero. Similar to the treatment of the structure solution for $Na_8Pb_2(Si_2Se_6)$ [5], the Eu(1) was partially occupied with Na(1), such that the sum of occupancies was set equal to full occupancy. After least-squares refinement, the relative occupancies refined to 49.8% Eu(1) and 50.2% Na(1), and the isotropic displacement parameter of the Eu(1)/Na(1) site dropped to 0.016 Å. This site was constrained to 50% Eu(1)/50% Na(1), which gave a charged-balanced formula. All of the atoms were refined anisotropically ($R_1 = 2.10\%$, $R_w = 4.93\%$). This solution is equivalent to the model shown in Fig. 2.

Table 2
Fractional atomic coordinates, equivalent isotropic displacement parameters (Å$^2 \times 10^3$), and fractional occupancies of $Na_8Eu_2(Si_2Se_6)_2$

	x	y	z	U (eq)[a]	Fractional occupation
Eu	0.5000	0.83409(5)	0.5000	17.8(2)	0.5
Na(1)	0.5000	0.83409(5)	0.5000	17.8(2)	0.5
Na(2)	0.5000	0.0000	0.0000	30.7(10)	
Na(3)	0.0000	0.1737(2)	0.0000	24.9(7)	
Si	0.0495(2)	0.0000	0.6535(2)	13.9(4)	
Se(1)	0.77593(9)	0.0000	0.74547(8)	18.2(2)	
Se(2)	0.23460(6)	0.15339(4)	0.74652(5)	17.6(2)	

[a] U (eq) is defined as one-third of the trace of the orthogonalized U_{ij} tensor.

2.3.2. $Na_9Sm(Ge_2Se_6)_2$ **II**

A block-like crystal of $Na_9Sm(Ge_2Se_6)_2$ with dimensions 0.1 mm × 0.1 mm × 0.1 mm was mounted on a glass fiber with epoxy. Cell constants were initially calculated from 120 frames of reflections, and the final cell constants were determined from a set of 2771 strong reflections obtained from data collection. An absorption correction was applied

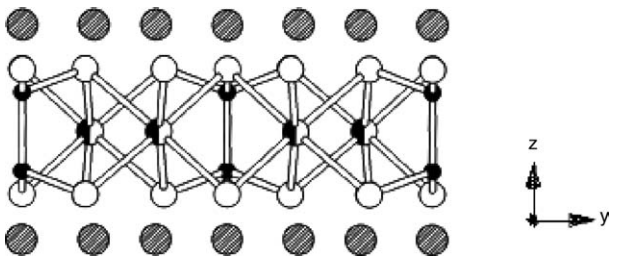

Fig. 2. Graphical representations of $Na_8Eu_2(Si_2Se_6)_2$ as viewed along the a crystallographic axis. The shared Eu/Na position is shaded black/white, Si is filled, Se is open and Na is crosshatched.

Table 3
Fractional atomic coordinates, equivalent isotropic displacement parameters ($Å^2 \times 10^3$), and fractional occupancies for $Na_9Sm(Ge_2Se_6)_2$

	x	y	z	U (eq)[a]	Fractional occupation
Na(1)	0.5000	0.6768(1)	0.5000	17(1)	0.75
Sm(1)	0.5000	0.6768(1)	0.5000	17(1)	0.25
Na(2)	0.5000	0.5000	1.0000	44(1)	
Na(3)	0	0.3457(3)	1.0000	38(1)	
Ge(1)	0.1596(1)	0.5000	0.5579(1)	14(1)	
Se(1)	0.2596(1)	0.5000	0.2775(1)	21(1)	
Se(2)	0.2500(1)	0.3419(1)	0.7502(1)	21(1)	

[a] U (eq) is defined as one-third of the trace of the orthogonalized U_{ij} tensor.

($R_{int} = 0.0556$) and all atoms were refined anisotropically on F^2 for 36 variables [11]. The systematic absences and Friedel pair comparisons again pointed clearly to the space group $C2/m$. Table 3 lists fractional coordinates and equivalent isotropic displacement parameters for $Na_9Sm(Ge_2Se_6)_2$, and Fig. 1b displays the coordination environment around the Sm(1) position with anisotropic displacement ellipsoids for all of the atoms.

Compound **II** was modeled as a structure occupational disorder at the Sm/Na site, similar to the disorder observed in the Eu/Na sites in **I**. The structure was initially refined with only Sm occupying the Sm(1)/Na(1) site. This solution was poor ($R_1/R_w = 0.1858/0.4576$); all of the atoms except Sm were non-positive definite upon anisotropic refinement, and the charge balance was unreasonable. When the occupancy of this site was allowed to refine freely, the occupancy refined to 0.391(2), equivalent to 24.2 electrons (final $R_1/R_w = 0.0209/0.0478$). Na(1) was shared at this position, and the occupancy for the shared site refined to 0.735(13) Na/0.264(3) Sm. The occupancy was then set to exactly 0.25 Sm and 0.75 Na in order to charge-balance the structure, yielding the reported formula. All of the atoms refined anisotropically without additional apparent disorder.

3. Results and discussion

$Na_8Eu_2(Si_2Se_6)_2$ **I**, is isostructural to the previously reported $Na_8Pb_2(Si_2Se_6)_2$, $Na_8Pb_2(Ge_2S_6)_2$ and $Na_8Sn_2(Ge_2S_6)_2$ [5]. Although this structure-type is not new, to our knowledge, **I** is the first structure containing both the $[Si_2Se_6]^{6-}$ unit and a rare earth element. $Na_8Eu_2(Si_2Se_6)_2$ is stable in air and in DMF for several weeks. Compound **I** is a two-dimensional structure with $^{\infty}[Eu_2(Si_2Se_6)_2]^{8-}$ layers separated by sodium cations. The staggered conformation of the ethane-like $[Si_2Se_6]^{6-}$ unit and pseudo-trigonal packing of the atoms in the layer is shown in Fig. 3a. The Eu(1)/Na(1), Na(2), Na(3) and Na(4) positions are all coordinated by selenium atoms in a slightly distorted octahedral arrangement. Selected bond distances and angles around the Eu and Si sites are reported in Table 4. The average Eu(1)–Se distance in the structure (Fig. 2) is 3.08 Å. Finally, referring to Table 1, we have found two other structures that are isostructural to this structure: $Na_8Eu_2(Ge_2Se_6)_2$ and $Na_8Eu_2(Si_2Te_6)_2$. These structures also display the Na/Eu site mixing and the Si–Si or Ge–Ge bond being perpendicular to the selenium layers, as seen in Fig. 2.

Table 4
Selected bond distances (Å) and angles (°) for $Na_8Eu_2(Si_2Se_6)_2$

Eu(1)—Se(1) × 2	3.0727(15)	Si(1)—Se(1)	2.280(4)
Eu(1)—Se(2) × 2	3.0811(14)	Si(1)—Se(2) × 2	2.291(3)
Eu(1)—Se(2′) × 2	3.0909(11)	Si(1)—Si(1′)	2.335(9)
		Si(2)—Se(2)	2.55(12)
		Si(2)—Se(1)	2.56(12)
		Si(2)—Se(2′)	2.67(11)
		Si(2)—Si(2)	2.0(3)
Se(1)—Eu(1)—Se(2)′ × 2	87.38(3)	Se(2)—Si(1)—Si(1)	107.50(15)
Se(2)—Eu(1)—Se(2)′ × 2	89.05(3)	Se(1)—Si(1)—Si(1)	108.33(2)
Se(2)′—Eu(1)—Se(2) × 2	96.91(3)	Se(2)—Si(1)—Se(2)	110.79(17)
Se(1)—Eu(1)—Se(1)′	97.19(4)	Se(1)—Si(1)—Se(2)	111.27(12)
Se(1)′—Eu(1)—Se(2)′ × 2	87.07(3)		
Se(2)′—Eu(1)—Se(2)	88.99(4)		
Se(2)′—Eu(1)—Se(2)′ × 2	86.96(3)		
		Se(1)—Si(2)—Se(2)	109(4)
		Se(2)—Si(2)—Se(2)	109(4)
		Se(2)—Si(2)—Se(1)	112(5)
		Si(2)—Si(2)—Se(2)	111(4)

$Na_9Sm(Ge_2Se_6)_2$ **II**, is not isostructural to **I**, but it is closely related to **I**. The primary difference between the two structures is the orientation of the M–M bonds (M = Si, Ge), and the coordination environments around these atoms. Fig. 3 displays a view of the two structures along equivalent axes, and the rotation of the Ge–Ge bonds from a perpendicular orientation in **I** (relative to the selenium layers) in Fig. 3a to a nearly horizontal orientation in **II** in Fig. 3b is obvious. This rotation is likely a steric effect caused by long bonds between Ge and Se, combined with the smaller size of Sm^{3+} relative to Eu^{2+}. Previous structures [5] isostructural to **I** were formed from either Si_2Se_6 or Ge_2S_6 units, each with shorter M–X (M = Pb, Sn; X = S, Se) bond distances. The pseudo-octahedral environments of $LnSe_6$ in both **I** and **II** are similar, when the Sm–Se bond lengths and angles in Table 5 are compared to the Eu–Se environments in Table 4. This implies that the distortive effects of the Si–Si bonds oriented along the c crystallographic axis in **I** are similar in magnitude to the effects of Ge–Ge bonds directed along a in **II**. The Sm–Se,

Table 5
Selected bond distances (Å) and bond angles (°) for $Na_9Sm(Ge_2Se_6)_2$

Sm—Se(1) × 2	3.0077(10)	Ge—Se(1)	2.3491(11)
Sm—Se(2) × 2	3.0176(9)	Ge—Se(2) × 2	2.3571(8)
Sm—Se(2′) × 2	3.0307(7)	Ge—Ge	2.4172(16)
Se(1)—Sm—Se(1)′	87.95(4)	Se(1)—Ge—Se(2)′ × 2	111.78(3)
Se(2)—Sm—Se(2)′ × 2	95.88(4)	Se(2)′—Ge—Se(2)	110.46(4)
Se(1)′—Sm—Se(2)′ × 2	88.12(2)	Se(1)—Ge—Ge′	106.80(5)
Se(1)′—Sm—Se(2)′ × 2	93.38(3)	Se(2)′—Ge—Ge′ × 2	107.91(5)
Se(1)—Sm—Se(2)′ × 2	80.37(3)		
Se(2)′—Sm—Se(2)′	97.65(3)		
Se(2)′—Sm—Se(2)′ × 2	88.15(2)		

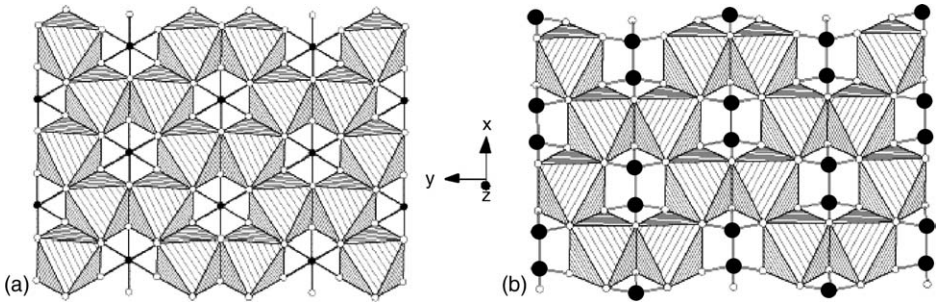

Fig. 3. Polyhedral representations of (a) $Na_8Eu_2(Si_2Se_6)_2$ and (b) $Na_9Sm(Ge_2Se_6)_2$ viewed perpendicular to the selenide layers. Shaded polyhedra represent $LnSe_6$ octahedra; the solid shaded spheres represent Si or Ge; the white spheres represent Se. The sodium atoms have been removed for clarity.

Ge–Se and Ge–Ge bond lengths in **II** are typical for these atoms.

I and **II** can be described as relatives of the MPS_3 structure (M = transition metal), which consists of layers of P_2S_6 and MS_6 octahedra separated by van der Waals gaps [15]. MPS_3 structures also crystallize in a monoclinic space group, and like the structures presented in this article, the chalcogens are nearly close-packed, and the structure retains pseudo-trigonal symmetry, although the organization of the atoms within the cell breaks this symmetry. The ideal β angle for a centered monoclinic cell to perfectly transform to a hexagonal cell is 107.16°. When **I** is compared to $FePS_3$, an MPS_3 structure with an ideal β angle, one finds that the unit cell of **I** is scaled 19% larger than $FePS_3$, and the β angle is slightly obtuse. The pseudo-hexagonal organization of the anions in **I** may be a clue to the origin of the disorder in this structure, since the β angle in **I** is the closest to ideal of any of the related published structures.

As a comparative study, we prepared related compounds listed in Table 1 to study the effects of the rare earth cation choice (La, Eu, Sm), the main group metal choice (Si, Ge) and the chalcogen choice (Se, Te). A summary of structural information can be found along with that for **I** and **II**. It should be noted that these other structures will not be described in detail here due to space considerations but will be submitted to the crystallographic database. As noted earlier, $Na_8Eu_2(Ge_2Se_6)_2$ and $Na_8Eu_2(Si_2Te_6)_2$ are isostructural to **I**. The compound $Na_9Sm(Si_2Se_6)_2$ is not isostructural with **II** because the Si–Si bond lies perpendicular to the planes as in **I**, yet the charge on the layers must be balanced by the stoichiometry Na/Sm = 9/1. However, $Na_9La(Ge_2Se_6)_2$ is isostructural to **II**, with the Ge–Ge bond lying parallel to the planes of the layers (as in Fig. 3b). We have evaluated the relative sizes of the rare earth ions, the chalcogen ions and the Si–Si and Ge–Ge units, yet we have not been able to decipher the trend that seems to drive the selection of the orientation of the pnictogen dimer in the layers.

4. Spectroscopic analysis

A table of Raman scattering peaks from $Na_8Eu_2(Si_2Se_6)_2$ and $Na_9Sm(Ge_2Se_6)_2$ is listed in Table 6. The Raman spectra are surprisingly similar to those collected from structures containing only simple $(MSe_4)^{4-}$ (M = Si, Ge) tetrahedra [16]. Since Raman spectroscopy on quaternary structures primarily provides information about the local environment around the silicon or germanium, this indicates that the M–M bond within a $(M_2Se_6)^{6-}$ unit does not significantly affect the vibrational behavior of that unit. Using other main group chalcogenides as a guide, the primary peak can be assigned to a pseudo-symmetric A1 stretching vibration of the $(M_2Se_6)^{6-}$ unit [16]. Lower energy peaks are due to unassigned bending modes, and the higher energy peaks are due to unassigned stretching modes. The peak at 237 cm^{-1} is a result of elemental selenium impurities that could not be removed from the sample.

Analysis of UV–vis diffuse reflectance data from **I** showed that this structure is a likely semiconductor with an optical band-gap of 2.15 eV. This value can be compared to the published band gaps of $K_2EuSiSe_5$ and $KEuSiSe_4$ of 2.00 and 1.72 eV, respectively [17]. These values are all within the expected range for a selenide semiconductor. Other selenides from Table 1 showed similar spectra.

Photoluminescence measurements of $Na_8Eu_2(Si_2Se_6)_2$ (Fig. 4) show that this material is an efficient phosphor with an emission at λ_{max} = 590 nm. The measured excitation and emission spectra are consistent with those from Eu^{2+} in similar environments. For example, Peters and Baglio found that europium-doped alkaline earth thiogallate phosphors displayed a broad emission peak centered at λ_{max} = 500–570 nm when excited at 350–370 nm [18]. Transitions between the $4f^6$ 5d and $4f^7$ energy levels were determined to be responsible for this luminescence, and the excitation and emission energies were sensitive to the chemical environment around

Table 6
Raman peaks (cm^{-1}) found for $N_8Eu_2(Si_2Se_6)_2$ and $Na_9Sm(Ge_2Se_6)_2$

$N_8Eu_2(Si_2Se_6)_2$	$Na_9Sm(Ge_2Se_6)_2$
129	125
153	159
208	187, A1
232, A1	234
237[a]	314
407	385

[a] Indicates peak due to elemental selenium impurities.

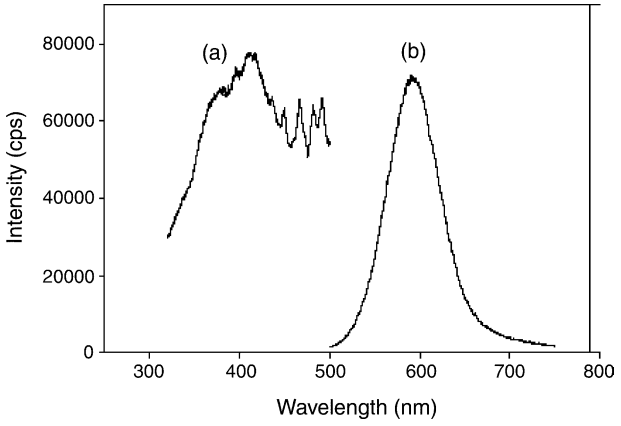

Fig. 4. (a) Excitation and (b) emission photoluminescence spectra of $Na_8Eu_2(Si_2Se_6)_2$.

Eu^{2+}. In a related study, Eu^{2+} doped in a CsS matrix exhibits a broad emission centered at $\lambda_{max} = 640$ nm when excited at 460 nm [19]. Since the oxidation state of europium in chalcogenide structures can be ambiguous resulting in improper assumptions based on charge balance, photoluminescence measurements are necessary for probing the electronic structure of europium-containing crystals. No evidence of Eu^{3+} was found in the compound through this study.

5. Conclusions

The general formula $A_9{}^{I}M_2{}^{II}(M_2{}^{IV}X_6)_2$ (A^I = Na, K; M^{II} = Eu, Pb, Sn; M^{IV} = Si, Ge; X = S, Se, Te) now represents a family of structurally related compounds containing interesting $M_2{}^{IV}X_6{}^{-6}$ building blocks where $Na_8Eu_2(Si_2Se_6)_2$ **I**, is a member of this family. $Na_9Sm(Ge_2Se_6)_2$ **II**, and $Na_9La(Ge_2Se_6)_2$ are at this time isolated examples of a related family of structures $A_9M^{III}(M_2{}^{IV}X_6)_2$ where (A^I = Na, K; M^{III} = Sm, La; M^{IV} = Si, Ge; X = Se) that possess the Ge–Ge unit parallel to the selenium layers. It is possible that a search through the rare earth series may reveal other compounds isostructural to **II**, but our current structural analysis shows the $Na_9(La/Sm)(Ge_2Se_6)_2$ is unique. We are currently exploring other quaternary alkali-rare earth-main group-chalcogenide systems in order to find new structures, and to better understand the chemical forces that stabilize complex main group chalcogenide units within these structures. Our goal is to develop a rational synthesis strategy for developing new quaternary structures. Understanding at this level would allow unprecedented control over the properties of new materials.

Acknowledgment

This work was supported by the National Science Foundation (CHE-0076180 and 0343412). The authors thank Susie Miller and Oren Anderson for their helpful discussions.

References

[1] K.O. Klepp, Z. Naturforsch., B: Anorg. Chem. Org. Chem. 40 (1985) 878–882.
[2] B. Eismann, E. Kieselbach, H. Schaefer, H. Schrod, Z. Anorg. Allg. Chem. 516 (1984) 49–54.
[3] B. Eisenmann, J. Hansa, Z. Kristallogr. 206 (1993) 101–102.
[4] P. Wu, J.A. Ibers, J. Solid State Chem. 107 (1993) 347–355.
[5] G.A. Marking, M.G. Kanatzidis, J. Alloys Compd. 259 (1997) 122–128.
[6] C.R. Evenson IV, P.K. Dorhout, Inorg. Chem. 40 (2001) 2875–2883.
[7] M.G. Kanatzidis, Chem. Mater. 2 (1990) 353–363.
[8] M.G. Kanatzidis, et al., unpublished results.
[9] G.M. Sheldrick, SAINT; Data Processing Software for the SMART System, Bruker Analytical X-ray Instruments, Inc., Madison, WI, 1995.
[10] G.M. Sheldrick, SADABS, University of Göttingen, Germany, 1997.
[11] G.M. Sheldrick, SHELXTL.PC Version 5.1, Bruker AXS Inc., Madison, WI, 1998.
[12] T.J. McCarthy, T.A. Tanzer, M.G. Kanatzidis, J. Am. Chem. Soc. 117 (1995) 1294–1301.
[13] C.R. Evenson, P.K. Dorhout, Inorg. Chem. 40 (2001) 2409–2414.
[14] F. Wilkinson, G. Kelly, in: J.C. Scaiano (Ed.), CRC Handbook of Organic Photochemistry, vol. 1, CRC Press, Boca Raton, FL, 1989, pp. 293–314.
[15] R. Brec, Solid State Ionics 22 (1986) 3–30.
[16] Z.V. Popovic, Fizika 15 (1983) 11–27.
[17] C.R. Evenson IV, P.K. Dorhout, Inorg. Chem. 40 (2001) 2409–2414.
[18] T.E. Peters, J.A. Baglio, J. Electrochem. Soc. 119 (1972) 230–236.
[19] J. Wu, D. Newman, I.V.F. Viney, J. Lumin. 99 (2002) 237–245.